AuAg bimetallic nanoparticles film fabricated based on H_2O_2-mediated silver reduction and its application

Li Wang, Fuan Wang, Li Shang, Chengzhou Zhu, Wen Ren, Shaojun Dong*

State Key Laboratory of Electroanalytical Chemistry, Changchun Institute of Applied Chemistry, Chinese Academy of Sciences, Renming Street 5625, Changchun, Jilin 130022, China

ARTICLE INFO

ABSTRACT

A method to fabricate AuAg bimetallic nanoparticles film by H_2O_2-mediated reduction of silver was reported. Gold nanoparticles (Au NPs) were first adsorbed onto the surface of a self-assembled 2-aminoethanethiol monolayer-modified gold film or 3-aminopropyltriethoxysilane (APTES) monolayer-modified quartz slide. Upon further treatment of this modified film with the solution containing silver nitrate ($AgNO_3$) and H_2O_2, silver was deposited on the surface of Au NPs. The size of the AuAg bimetallic particles could be readily tuned by manipulating the concentration of H_2O_2. Surface plasmon resonance (SPR) was used to investigate the process, the deposition of silver on Au NPs modified gold film resulted in an obvious decrease of depth in the SPR reflectance intensity and minimum angle curves (SPR R-θ curves), which may be utilized for the quantitative SPR detection of the analyte, H_2O_2. Combination of the biocatalytic reaction that could yield H_2O_2 by using the enzyme, glucose oxidase, with the deposition of silver may enable the design of a glucose biosensor by SPR technique. Furthermore, we evaluated the AuAg bimetallic nanoparticles film for their ability to be an effective substrate for surface-enhanced Raman scattering (SERS).

1. Introduction

In recent years, bimetallic nanomaterials have been an attractive area of research within nanobiotechnology for their unusual optical [1,2], catalytic [3], and magnetic properties [4]. In this regard, Au–Ag bimetallic nanostructures have gained increasing attention with their optical properties, including light absorption, elastic light scattering, and inelastic light scattering (e.g., surface-enhanced Raman scattering) [2,5]. Such structures have been studied for potential analytical and biomedical applications [6]. Synthetic strategies utilized to make such nanostructures include simultaneous chemical reduction of two or more metal ions [7], reduction of one metal ion on the surface of another metal particle [8,9], and radiation chemistry [10].

In this study, we developed a simple method to fabricate AuAg bimetallic nanoparticles film based on H_2O_2-mediated reduction of silver. Gold nanoparticles (Au NPs) were chosen as the cores, H_2O_2 was used as an active reducing agent for the reduction of silver on the surface of Au NPs to form AuAg bimetallic nanoparticles. The size of the AuAg bimetallic nanoparticles could be tuned by manipulating the conditions. The deposition of silver on Au NPs modified surface plasmon resonance (SPR) gold film resulted in an obvious decrease of depth in the SPR reflectance intensity and minimum angle curves (SPR R-θ curves). This effect may be utilized for a SPR sensor to detect the analyte, H_2O_2. The obtained film may be also used as a good surface-enhanced Raman scattering (SERS) active substrate, which could be further developed to construct a useful sensing platform for the detection of analytes such as some biologically important molecules.

2. Experimental

2.1. Reagents

2-Aminoethanethiol, sodium tetrahydroborate ($NaBH_4$), 3-aminopropyltriethoxysilane (APTES), 4-aminothiophenol (4-ATP), and N′-a-hydroxythylpiperazine-N′-ethanesulfanic acid (HEPES) were obtained from Aldrich. Hydrogen peroxide (H_2O_2), silver nitrate ($AgNO_3$), hydrogen tetrachloroaurate ($HAuCl_4 \cdot 3H_2O$), and sodium citrate were obtained from Beijing Chemical Co. (China). All of the other chemicals, unless mentioned otherwise, were of analytical grade and were used as received.

2.2. SPR measurements

SPR measurements were performed with a home-built SPR system [11]. It was based on the Kretschmann configuration to achieve the resonant condition by attenuated total internal reflec-

* Corresponding author. Tel.: +86 431 5262101; fax: +86 431 5689711.
E-mail addresses: dongsj@ciac.jl.cn, dengliu@ciac.jl.cn (S. Dong).

tion spectroscope (ATR). For further experiments, the gold SPR film (thickness = 47.4 nm) cleaned through piranha solution was pressed onto the base of a half-cylindrical lens (ZK$_7$, n = 1.61) via an index matching oil (n = 1.61). Linearly p-polarized light having a wavelength of 670 nm from a diode laser was directed through the prism onto the SPR gold film. The intensity of the reflected light was measured as a function of the angle of incidence (θ). The gold surface of the glass slide was mounted against the Teflon cell with use of a Kalrez O-ring (the apparent area was 0.38 cm^2).

2.3. Preparation of Au NPs and the Au NPs modified film

Au NPs (about 3 nm) were prepared using NaBH$_4$ and stabilized with sodium citrate according to the literature [12]. In brief, 0.5 mL of 1% aqueous HAuCl$_4$·3H$_2$O was added to 50 mL water with vigorous stirring, followed by the addition of 0.5 mL of 1% aqueous sodium citrate 1 min later. After an additional 1 min, 0.5 mL of 0.075% NaBH$_4$ in 1% sodium citrate was added, and the solution color changed from colorless to orange. The solution was stirred for another 10 min, and then stored at 4 °C prior to use. The formation of Au NPs was examined using the UV–vis spectrum, which produced a strong surface plasmon band at 508 nm (not shown) characteristic of monodispersed colloidal Au. Au NPs were also characterized by transmission electron microscopy (Fig. 1S).

Quartz slide or SPR gold film was used as the substrate for preparing the Au NPs modified film. Quartz slide or SPR gold film was first immersed in APTES (10% in methanol) or 2-aminoethanethiol aqueous solution (0.01 M) for 12 h to form positively charged surface. After washing and N$_2$ drying, the substrate was soaked in the negatively charged Au NPs aqueous solution for 2 h, and rinsed in water.

2.4. Reduction of silver on the Au NPs modified film

The Au NPs modified film was immersed in the deposition solution consisted of 40 mM AgNO$_3$ (in 0.01 M HEPES buffer, pH 7.0) and H$_2$O$_2$ (in 0.01 M HEPES buffer, pH 7.0) at 30 °C for 30 min. Then, the film was washed with water sequentially.

Enzyme reaction involved reduction of silver on the Au NPs modified SPR gold film was also performed. A solution of HEPES buffer (0.01 M, pH 7.0) that contained GOx (2 mg/mL), and different concentrations of glucose was allowed to react for 30 min at 30 °C, then, 0.5 mL of the above solution and 0.5 mL of 80 mM AgNO$_3$ were added in Teflon cell, respectively, and reacted at 30 °C for 30 min. Afterwards, SPR cell was washed with buffer and water.

2.5. SERS measurements of 4-ATP on the AuAg bimetallic nanoparticles films

50 μL of 10 μM 4-ATP aqueous solution was dropped onto the as-prepared AuAg bimetallic nanoparticles films, and the solvent was allowed to evaporate under ambient conditions. Finally, a Raman spectrometer was used to measure the SERS activities of these films. All of the Raman spectra were recorded in 10 s. All the spectra were baseline corrected and noise filtered.

2.6. Other instruments

UV–vis absorption spectra were recorded with a Cary 500 UV–vis–NIR spectrometer (Varian, USA). X-ray photoelectron spectroscopy (XPS) measurements were carried out on an ES-CALAB-MKII spectrometer (VG Co., U.K.) with Al Kα X-ray radiation as the X-ray source for excitation. The morphology of the samples was inspected using a scanning electron microscope (SEM,
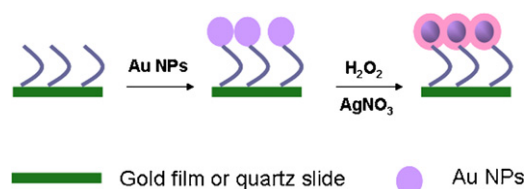

Fig. 1. Schematic illustration for the fabrication process of the AuAg bimetallic nanoparticles film.
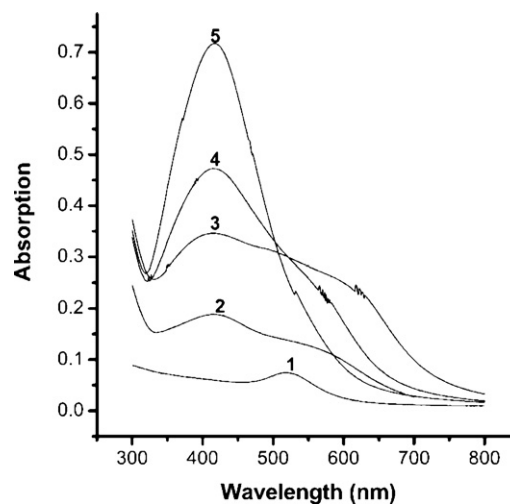

Fig. 2. Absorption spectra of the Au NPs modified quartz slides before (1) and after the deposition of silver on the Au NPs modified films in the presence of H$_2$O$_2$: 0.2 mM (2), 0.4 mM (3), 0.6 mM (4), and 1.0 mM (5).

S-4800, Hitachi, Japan). Transmission electron microscopy (TEM) observations were carried out on a JEM-1011 microscope operating at 100.0 kV. SERS spectra were measured with a Renishaw 2000 model confocal microscopy Raman spectrometer with a CCD detector and a holographic notch filter (Renishaw Ltd., Gloucestershire, U.K.). Radiation of 514.5 nm from an air-cooled argon ion laser was used for the SERS excitation.

3. Results and discussion

3.1. Characterization of the AuAg bimetallic nanoparticles films by UV–vis, SEM and XPS

The AuAg bimetallic nanoparticles films were fabricated as schematically outlined in Fig. 1. In brief, Au NPs were confined onto the surface of a self-assembled 2-aminoethanethiol monolayer-modified gold film or APTES monolayer-modified quartz slide, and then, H$_2$O$_2$-mediated reduction of silver was introduced to form the AuAg bimetallic nanoparticles.

The optical properties of the fabricated AuAg bimetallic nanoparticles films were further recorded by UV–vis spectroscopy shown in Fig. 2. The monolayer of Au NPs assembled on quartz slides showed characteristic surface plasmon peak of Au NPs, which was red-shifted to 513 nm due to the coupling of the Au NPs on the film. With the silver reduction, the new peak at about 415 nm corresponding to the surface plasmon excitation of silver appeared, which may indicate that the Au NPs were mostly covered by silver. Two peaks at 415 and 600 nm were observed for the fabricated AuAg bimetallic nanoparticles film (curves 2 and 3). Further increasing the concentration of H$_2$O$_2$, the SPR band of Au disappeared and the SPR band of silver at about 415 nm increased gradually. The appearance of only one absorption band may be attributed to that silver shell was very thick compared to Au NPs,

therefore it showed only one plasmon resonance corresponding to silver.

To further understand the reduction of silver, SEM analysis of the Au NPs modified gold surfaces upon the reduction of silver was performed. Fig. 3 showed the SEM images of the Au NPs modified SPR gold film surface before (A) and after the reduction of Ag in the presence of 0.2 mM (B) and 0.6 mM (C) H_2O_2. Fig. 3A showed that the Au NPs were almost invisible prior to the catalytic reduction of silver. After the reduction process in the presence of 0.2 mM H_2O_2, nanoparticles with the size of 16–19 nm were observed, although the particles were not very clear. The diameter of these small particles became larger as the concentration of H_2O_2 was increased. After the reduction of silver on the Au NPs in the presence of 0.6 mM H_2O_2, larger nanoparticles with the size of 18–23 nm were observed. In addition, the surface coverage was also increased. Obviously, the concentration of H_2O_2 had an important influence on the size of the particles. More silver atoms were deposited on the surface of Au NPs as the concentration of H_2O_2 increased, which agreed with the absorption spectra results. Au NPs modified gold films upon the silver reduction by H_2O_2 were also characterized by means of XPS (Fig. 2S). XPS results indicated that the Ag content in the SPR film was dependent of the concentration of the H_2O_2 used, more silver atoms were deposited on the surface of Au NPs as the concentration of H_2O_2 increased, which was consistent with the analysis of the optical spectra and SEM images discussed above.

3.2. SPR measurements

SPR is one of the most exciting surface-sensitive techniques for detecting analytes adsorbed on a metal surface [13–16]. The change in the thickness of the metal film would result in large change in the depth of the SPR R-θ curves. SPR measurements were performed here in order to characterize the fabrication process of the AuAg bimetallic nanoparticles film. Fig. 4 showed the SPR R-θ curves in situ recorded after various surface modification steps. As indicated in Fig. 4, the SPR minimum reflectivity angle was shifted to higher angle after adsorption of 2-aminoethanethiol and Au NPs. The assembly of 2-aminoethanethiol on SPR gold film showed an angle shift of 0.18°. The value of angle shift was mainly dependent on the molecular weight and surface coverage of the molecule adsorbed on the SPR gold film. The assembly of Au NPs resulted in an angle shift of 0.8° and the depth of SPR R-θ curve was decreased after adsorption Au NPs. It is well known that SPR angle could be increased by Au NPs due to the electronic coupling interaction between the localized surface plasmon of Au NPs and the surface plasmon wave associated with the SPR gold film, and this electronic coupling interaction is strongly affected by the diameter of Au NPs. We also followed the H_2O_2-mediated reduction of silver by in situ SPR measurements. After H_2O_2-mediated reduction of silver in solution containing 40 mM $AgNO_3$ and 1.2 mM H_2O_2 in Teflon cell for 30 min, silver was deposited on the surface of Au NPs modified SPR gold film. The curve 4 in Fig. 4 showed the SPR R-θ curve after H_2O_2-mediated reduction of silver. The deposition of silver was accompanied by an obvious decrease of depth in SPR R-θ curve. We demonstrated that the reduction of silver on SPR gold film would result in an obvious decrease of depth in SPR R-θ curve. Control experiments showed no change of depth in SPR R-θ curves in the absence of Au NPs on the surface or in the absence of H_2O_2.

Fig. 5 showed the SPR R-θ curves of Au NPs modified SPR gold film resulting from the catalytic reduction of silver upon treatment with different concentrations of H_2O_2. The SPR R-θ curves were recorded after reduction of silver on Au NPs modified SPR gold film in the solution containing $AgNO_3$ and different concentrations of H_2O_2 for 30 min. As seen, with increasing the concentration of H_2O_2, the depth of SPR R-θ curves obviously decreased due to the
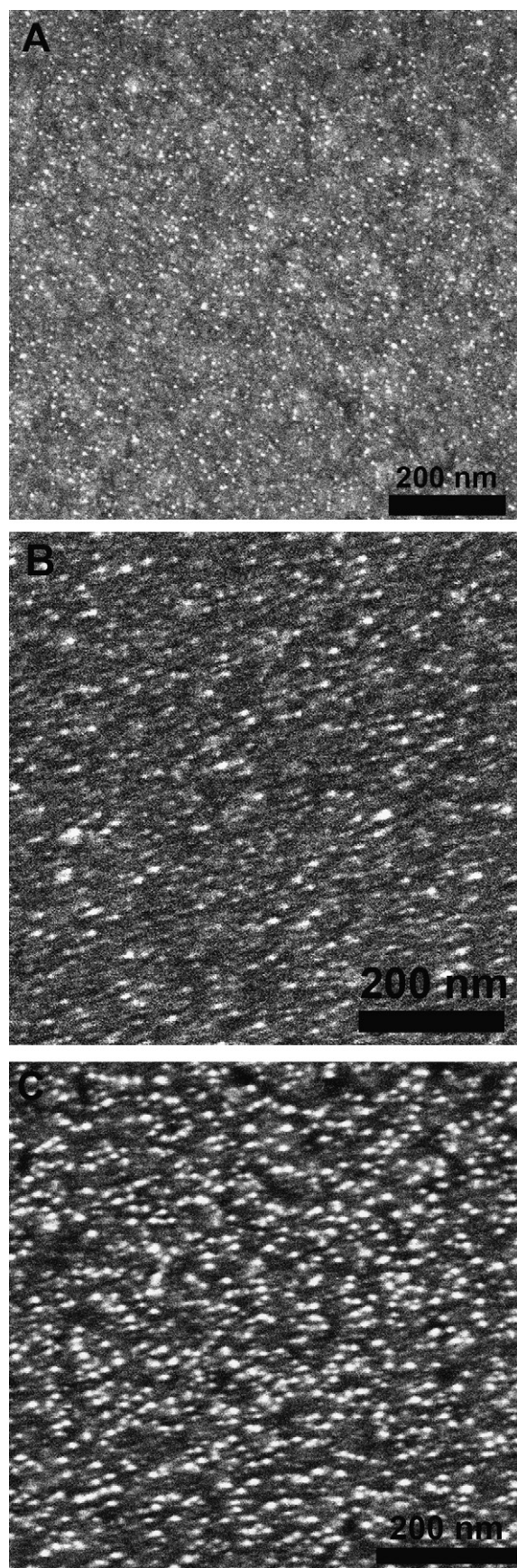

Fig. 3. SEM images of the Au NPs modified SPR gold films surface before (A) and after the deposition of silver on the Au NPs modified SPR gold film in the presence of H_2O_2: 0.2 mM (B) and 0.6 mM (C).
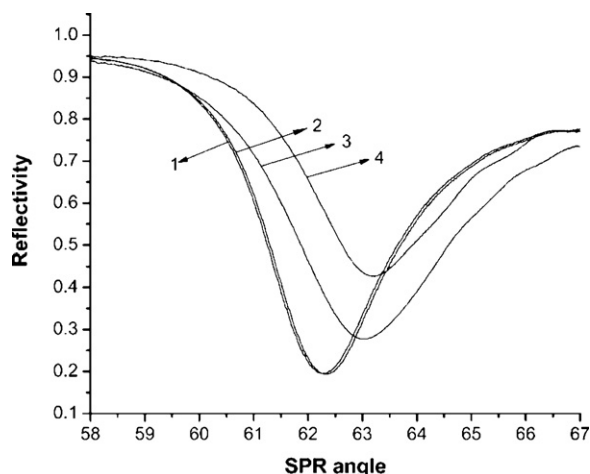
Fig. 4. SPR spectra in situ recorded after various surface modification steps: (1) the bare SPR gold film; (2) adsorbed 2-aminoethanethiol on the bare gold film; (3) adsorbed Au NPs on the gold film modified with 2-aminoethanethiol; (4) after depositing silver on the surface of Au NPs modified SPR gold film by the solution containing 1.2 mM H_2O_2 and 40 mm $AgNO_3$ for 30 min. All curves were recorded in pure water.
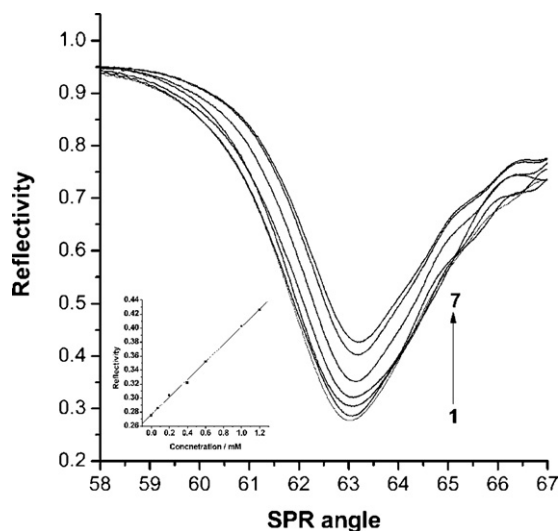

Fig. 5. SPR spectra after the deposition of silver upon treatment with 40 mM $AgNO_3$ and different concentrations of H_2O_2: (1) 0 mM, (2) 0.07 mM, (3) 0.2 mM, (4) 0.4 mM, (5) 0.6 mM, (6) 1.0 mM, and (7) 1.2 mM. All spectra were recorded in water after a reaction time of 30 min. Insert: calibration plots of the minimum reflectivity associated with the silver deposited in the presence of different concentrations of H_2O_2.

more silver deposited on Au NPs. Upon increasing the concentration of H_2O_2 from 0.07 to 0.2, 0.4, 0.6, 0.8 and 1.2 mM, the depth in SPR R-θ curves gradually changed from 0.287 to 0.301, 0.320, 0.351, 0.371, and 0.424, respectively. The insert of Fig. 5 showed the derived calibration curve. Obviously, with increasing concentration of H_2O_2, more silver atoms were deposited on SPR gold film. When more silver atoms were deposited on gold film, the depth of the SPR R-θ curves became smaller. The change in the depth of the SPR R-θ curves was mainly dependent on the thickness of the metal film.

Fig. 3S showed the depth change of SPR R-θ curves resulting from the silver reduction in the presence of H_2O_2 generated by GO*x* in the presence of different concentrations of glucose. As expected, the depth of SPR R-θ curves decreased as the concentration of glucose was elevated. It was noticeable that the change trend in the depth of SPR R-θ curves reduced when the concentrations of glucose further increased, which might be due to that the active sites
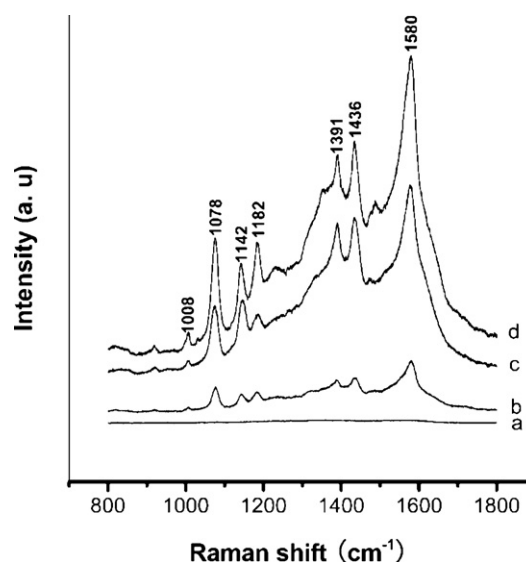

Fig. 6. SERS spectra of 10^{-5} M of 4-ATP on AuAg bimetallic nanoparticles films prepared by different concentrations of H_2O_2: (b) 0.2 mM, (c) 0.4 mM, (d) 0.6 mM. (a) Normal Raman spectrum of 4-ATP in a bare quartz slide.

of GO*x* units gradually became saturated at those glucose level. Control experiments revealed that O_2, glucose oxidase, and glucose were all essential to the catalytic deposition of silver, since the deposition of silver did not proceed if O_2, glucose oxidase, or glucose was excluded from the solution. These results clearly indicated that the primary generation of H_2O_2, which acted as the reducing agent, was essential to the deposition of silver.

3.3. Application of the AuAg bimetallic nanoparticles films in SERS

SERS has been shown to be a powerful tool for the detection of low concentration analytes [17,18]. In this regard, fabricating good SERS active substrates is of particular importance and has received intense interest in recent years. Here we showed that the as-fabricated AuAg bimetallic nanoparticles film could be readily used as a SERS substrate for molecular sensing with high sensitivity. 4-ATP, a kind of probe molecules commonly used in SERS studies, was investigated in the present work. Fig. 6 displayed the SERS spectrum of 4-ATP (curves b–d) on the AuAg bimetallic nanoparticles films. For comparison, the normal Raman spectrum of solid 4-ATP (curve a) was also presented. As shown, the intensities of four b_2 modes at 1580, 1436, 1391, and 1142 cm^{-1} and one a_1 mode at 1078 cm^{-1} on the AuAg bimetallic nanoparticle films (curves b–d) increased compared with those in the Raman spectrum of solid 4-ATP (curve a). The corresponding intensity of the b_2 mode increased, which was associated with the charge transfer of the metal to the adsorbed molecules. The observed large enhancement also suggested that the as-prepared nanocomposite films could indeed serve as robust substrates for carrying out molecular sensing with high sensitivity and specificity.

4. Conclusion

In conclusion, the present study has demonstrated the H_2O_2-mediated silver reduction on the surface of Au NPs to fabricate AuAg bimetallic nanoparticles film. H_2O_2-mediated silver reduction has been employed in the design of surface plasmon resonance (SPR) biosensors. The deposition of silver on Au NPs modified gold film resulted in an obvious decrease of depth in the SPR reflectance intensity and minimum angle curves (SPR R-θ curves), and the depth change of SPR R-θ curves mainly relied on the

amount of silver deposited on gold film that can be controlled by the concentration of H_2O_2. This effect is suggested to be suitable for a SPR sensor for H_2O_2. Furthermore, by combining the biocatalytic reaction of the substrate by the corresponding enzyme, for example, glucose oxidase, with the deposition of silver, a glucose biosensor can be fabricated. It was also shown that the AuAg bimetallic nanoparticles film may be used as a good substrate for SERS.

Acknowledgements

Appendix A. Supplementary data

Supplementary data associated with this article can be found, in the online version, at doi:10.1016/j.talanta.2010.04.009.

References

[1] S. Pande, S.K. Ghosh, S. Praharaj, S. Panigrahi, S. Basu, S. Jana, A. Pal, T. Tsukuda, T. Pal, J. Phys. Chem. C 111 (2007) 10806.
[2] S. Pande, S. Jana, A.K. Sinha, S. Sarkar, M. Basu, M. Pradhan, A. Pal, J. Chowdhury, T. Pal, J. Phys. Chem. C 113 (2009) 6989.
[3] J.F. Huang, S. Vongehr, S.C. Tang, H.M. Lu, J.C. Shen, X.K. Meng, Langmuir 25 (2009) 11890.
[4] Y.M. Zhai, J.F. Zhai, Y.L. Wang, S.J. Guo, W. Ren, S.J. Dong, J. Phys. Chem. C 113 (2009) 7009.
[5] S. Saha, A. Pal, S. Pande, S. Sarkar, S. Panigrahi, T. Pal, J. Phys. Chem. C 113 (2009) 7553.
[6] L.B. Yang, G.Y. Chen, J. Wang, T.T. Wang, M.Q. Li, J.H. Liu, J. Mater. Chem. 19 (2009) 6849.
[7] M.P. Mallin, C.J. Murphy, Nano Lett. 2 (2002) 1235.
[8] Q.B. Zhang, J.P. Xie, J.Y. Lee, J.X. Zhang, C. Boothroyd, Small 4 (2008) 1067.
[9] B. Rodriguez-Gonzalez, A. Burrows, M. Watanabe, C.J. Kiely, L.M. Liz-Marzan, J. Mater. Chem. 15 (2005) 1755.
[10] J.H. Hodak, A. Henglein, M. Giersig, G.V. Hartland, J. Phys. Chem. B 104 (2000) 11708.
[11] X.F. Kang, G.J. Cheng, S.J. Dong, Electrochem. Commun. 3 (2001) 489.
[12] Y.D. Jin, X.F. Kang, Y.H. Song, B.L. Zhang, G.J. Cheng, S.J. Dong, Anal. Chem. 73 (2001) 2843.
[13] X.F. Kang, Y.D. Jin, G.J. Cheng, S.J. Dong, Langmuir 18 (2002) 1713.
[14] T. Kang, S. Hong, I. Choi, J.J. Sung, Y. Kim, J.S. Hahn, J. Yi, J. Am. Chem. Soc. 128 (2006) 12870.
[15] L. He, M.D. Musick, S.R. Nicewarner, F.G. Salinas, S.J. Benkovic, M.J. Natan, C.D. Keating, J. Am. Chem. Soc. 122 (2000) 9071.
[16] C.F. Grant, V. Kanda, H. Yu, D.R. Bundle, M.T. McDermott, Langmuir 24 (2008) 14125.
[17] T. Wang, X.G. Hu, J.L. Wang, S.J. Dong, Talanta 75 (2008) 455.
[18] Y.J. Sun, L.L. Sun, B.H. Zhang, F.G. Xu, Z.L. Liu, C.L. Guo, Y. Zhang, Z. Li, Talanta 79 (2009) 562.